

Brillouin scattering, piezobirefringence, and dispersion of photoelastic coefficients of CdS and ZnO

Berkowicz, R.; Skettrup, Torben

Published in:
Physical Review B Condensed Matter

Link to article, DOI:
[10.1103/PhysRevB.11.2316](https://doi.org/10.1103/PhysRevB.11.2316)

Publication date:
1975

Document Version
Publisher's PDF, also known as Version of record

[Link back to DTU Orbit](#)

Citation (APA):
Berkowicz, R., & Skettrup, T. (1975). Brillouin scattering, piezobirefringence, and dispersion of photoelastic coefficients of CdS and ZnO. *Physical Review B Condensed Matter*, 11(6), 2316-2326. DOI: 10.1103/PhysRevB.11.2316

DTU Library

Technical Information Center of Denmark

General rights

Copyright and moral rights for the publications made accessible in the public portal are retained by the authors and/or other copyright owners and it is a condition of accessing publications that users recognise and abide by the legal requirements associated with these rights.

- Users may download and print one copy of any publication from the public portal for the purpose of private study or research.
- You may not further distribute the material or use it for any profit-making activity or commercial gain
- You may freely distribute the URL identifying the publication in the public portal

If you believe that this document breaches copyright please contact us providing details, and we will remove access to the work immediately and investigate your claim.

Brillouin scattering, piezobirefringence, and dispersion of photoelastic coefficients of CdS and ZnO

R. Berkowicz* and T. Skettrup

Physics Laboratory III, Technical University of Denmark, DK-2800 Lyngby, Denmark

(Received 30 September 1974)

We have measured the dispersion of the Brillouin scattering from acoustoelectrical domains in CdS and ZnO. These spectra are compared with the birefringence spectra obtained by applying uniaxial stress. The resonant cancellation of the Brillouin scattering occurs at the spectral position of the isotropic point of the stress-induced birefringence. From these spectra it is concluded that the Brillouin scattering in CdS and ZnO is determined by elasto-optic effects alone. The spectra of some of the photoelastic coefficients have been determined. A model dielectric constant is derived where both ground-state excitons and unbound continuum exciton states contribute. From this dielectric constant and the quasicubic model we calculate all the six independent photoelastic coefficients. By comparison with the experimental results the shear deformation potentials of the valence bands are obtained. It is found that the exchange interaction between the excitons may change the values of the photoelastic coefficients in ZnO about 10%.

I. INTRODUCTION

Resonant Brillouin scattering from acoustoelectric phonon domains has recently been observed in CdS and ZnO.¹ Both resonant enhancement and resonant cancellation of the scattering were found. From comparison between the scattering from piezoelectrically active and inactive phonon domains it was concluded that electro-optic effects are unimportant in the scattering mechanism, thus indicating that elasto-optic effects dominate. Elasto-optic effects in crystals are often described in terms of the photoelastic (elasto-optic) coefficients.² The purpose of the present work is to determine some of these coefficients and their spectral behavior, namely p_{44} and p_{66} , which are involved in the Brillouin scattering from acoustoelectric domains.

Tell, Worlock, and Martin³ have measured relative values of the photoelastic coefficients p_{11} , p_{12} , and p_{31} in CdS and ZnO by a Brillouin scattering method. Yu and Cardona⁴ have investigated the elasto-optic effects in CdS and ZnO by static stress-induced birefringence (piezobirefringence). They obtained coefficients related to p_{66} , and combinations of p_{11} , p_{13} , p_{31} , and p_{33} . Photoelastic coefficients for CdS at the He-Ne laser wavelength have also been obtained from Brillouin scattering.⁵ Here, we determine p_{66} and p_{44} for CdS and ZnO both from Brillouin scattering and from piezobirefringence measurements. It is the first time that the absolute values of the p_{44} spectrum are reported. The absolute values of p_{66} are in good agreement with those obtained by Yu and Cardona.⁴ Kohn⁶ has made a calculation of the photoelastic coefficients in CdS and ZnO, but neglected here the shear deformation potentials and the presence of

the third valence bands. Yu and Cardona⁴ also computed coefficients related to the photoelastic coefficients in CdS and ZnO. They found that exciton effects are important for the dispersion of the photoelastic coefficients for these materials and made semiquantitative fits to their measurements. Unfortunately, it was not possible to derive the values of the deformation potentials from the fits.

We have extended the theory of Yu and Cardona⁴ to include the effect of the unbound continuum exciton states above the fundamental band edge. We calculate all the six independent components of the photoelastic tensor, and we are able to derive values for the shear deformation potentials of CdS and ZnO by fitting to the experimental results.

II. PHOTOELASTIC COEFFICIENTS

The photoelastic coefficients p_{ijkl} are the components of a fourth-rank tensor \underline{p} defined by the equation²

$$\Delta(1/\underline{\epsilon}) = \underline{p} \cdot \underline{e} , \quad (1)$$

where $1/\underline{\epsilon}$ is the reciprocal of the tensor of the dielectric constant, and \underline{e} is the strain tensor. In the coordinate system where $\underline{\epsilon}$ is diagonal (without applied strain) the following relations are valid⁶:

$$\Delta\{1/\epsilon\}_{ij} = -\Delta\epsilon_{ij}/\epsilon_{ii}\epsilon_{jj} . \quad (2)$$

The definition of the photoelastic coefficients may then be written

$$p_{ijkl} = -\frac{1}{\epsilon_{ii}\epsilon_{jj}} \frac{\partial \epsilon_{ij}}{\partial e_{kl}} , \quad (3)$$

or with abbreviated suffixes,²

$$p_{mn} = -\frac{1}{2\epsilon_{ii}\epsilon_{jj}} \frac{\partial \epsilon_{ij}}{\partial e_{kl}} (1 + \delta_{kl}), \quad (3a)$$

where m and n represent ij and kl , respectively, according to the rules 11 → 1, 22 → 2, 33 → 3, 23 → 4, 13 → 5, 12 → 6.

In wurtzite structure only six independent p coefficients exist. These are $p_{11} = p_{22}$, $p_{12} = p_{21}$, $p_{13} = p_{23}$, $p_{31} = p_{32}$, p_{33} , $p_{44} = p_{55}$. Furthermore, $p_{66} = \frac{1}{2}(p_{11} - p_{12})$, while the remaining coefficients are zero.

III. EXPERIMENTAL RESULTS

Tell *et al.*³ measured the dispersion of p_{11} , p_{12} , and p_{31} for ZnO and CdS. Yu and Cardona⁴ determined essentially p_{66} and combinations of p_{11} , p_{13} , p_{31} , and p_{33} . Berkowicz and Price¹ reported the intensity of the Brillouin scattering which is closely connected with p_{44}^2 . Here, we have measured p_{66} and p_{44} both by the Brillouin scattering methods and by the piezobirefringence method. The Brillouin scattering measurements were performed as in Ref. (1). For CdS, furthermore, we also applied another geometry with phonon domains polarized and propagating perpendicular to the

c axis. This geometry was obtained by mode conversion in a domain reflected from the contact. Then the intensity of the scattered light depends on p_{66}^2 . We have not found ZnO crystals with propagating domains in this geometry.

The results for p_{44}^2 and p_{66}^2 from the Brillouin scattering measurements are shown in Figs. 1–4. It is seen that the dispersion of p_{66} is very similar to that of p_{44} . It should also be noted that the resonant cancellation of the Brillouin scattering occurs at the same wavelength (5635 Å for CdS) for both p_{44} and p_{66} within the experimental accuracy.

The photoelastic coefficients p_{44} and p_{66} may also be determined from measurements of the birefringence induced by an applied static uniaxial stress. We have done this for two different geometries. Uniaxial stress X perpendicular to the c axis ($\vec{X} \perp \vec{c}$) and light direction \vec{k} parallel to the c axis ($\vec{k} \parallel \vec{c}$) yields p_{66} ; stress direction at a certain angle α (30° or 45°) with respect to the c axis and $\vec{k} \perp \vec{c}$ yields p_{44} .

The samples were cut corresponding to the two kinds of geometries. They were polished and placed between crossed polarizers, and the spectral dependence of the transmission was recorded at room temperature. If the polarizer direction forms an angle ϕ with the (induced) optical axis of the crystal, the intensity I_T of the light transmitted

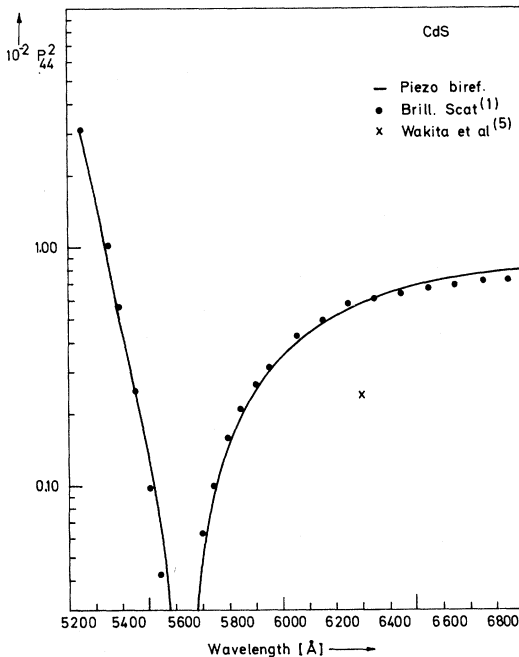


FIG. 1. p_{44}^2 for CdS obtained from stress measurements (solid line) and Brillouin scattering (dots). Absolute values of p_{44}^2 were determined from the stress results. Brillouin scattering results are here and in the following figures normalized to fit these absolute values. Wavelength of the resonant cancellation point is 5635 Å.

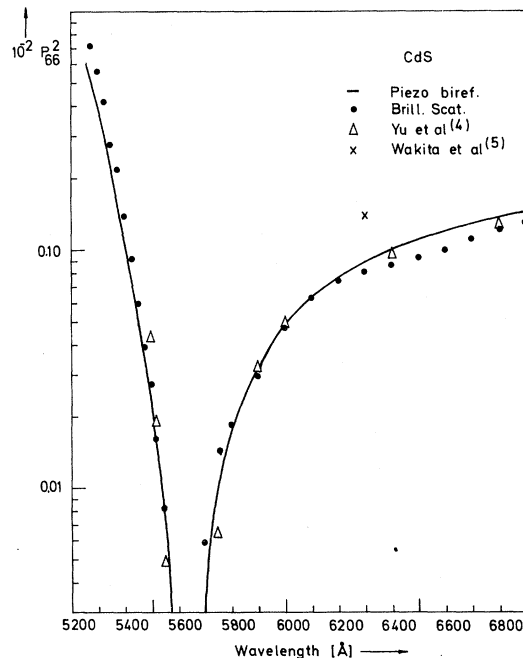


FIG. 2. p_{66}^2 for CdS obtained from stress measurements (solid line) and Brillouin scattering (dots). Results of Yu *et al.* are also shown (triangles). Wavelength of the resonant cancellation point is 5635 Å.

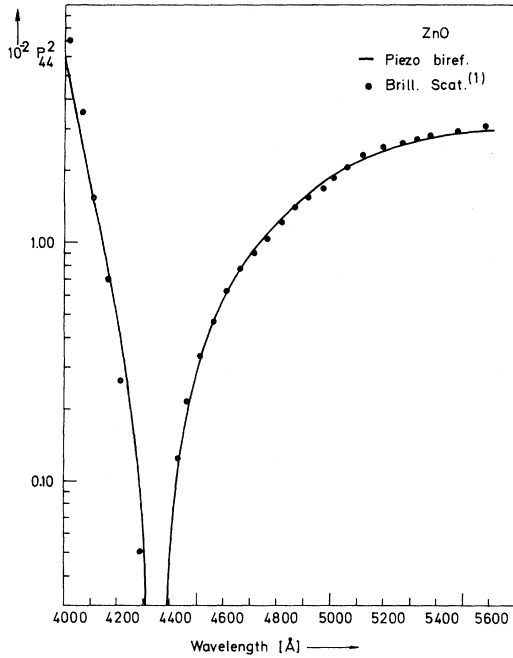


FIG. 3. p_{44}^2 for ZnO obtained from stress measurements (solid line) and Brillouin scattering (dots). Wavelength of the resonant cancellation point is 4328 Å.

through the crystal with thickness d is given by the equation

$$I_T = I_0 \sin^2(2\phi) \sin^2(\Delta n \pi d / \lambda), \quad (4)$$

where I_0 and λ are intensity and wavelength of the incoming light, and Δn is the difference between the refractive indices for light polarized parallel and perpendicular to the optical axis, respectively. For the isotropic geometry $\vec{X} \perp \vec{c}$ and $\vec{k} \parallel \vec{c}$ it is shown in Appendix A that

$$\Delta n = \frac{1}{2} \epsilon_{11}^{3/2} p_{66} S_{66} X, \quad (5)$$

where X is the uniaxial stress applied and $S_{66} = 2(S_{11} - S_{12})$ is a compliance constant. p_{66} may thus be determined from the intensity (4) of the transmitted light (where $\phi = 45^\circ$). For the anisotropic geometry where X forms the angle α with c and $\vec{k} \perp \vec{c}$, the crystal is already birefringent. The effect of the strain e_{13} is, to first order, to change the direction of the optical axis. As shown in Appendix A the angle θ between the directions of the optical axis with and without strain is given by

$$\tan 2\theta = \frac{2\epsilon_{11}\epsilon_{33}p_{44}e_{13}}{\epsilon_{33} - \epsilon_{11}} = \frac{\epsilon_{11}\epsilon_{33}p_{44}S_{44}\sin(2\alpha)X}{\epsilon_{33} - \epsilon_{11}}, \quad (6)$$

where S_{44} is a compliance constant, and α is the angle between X and c . In determining p_{44} , (4) and (6) are utilized. Two spectra are recorded.

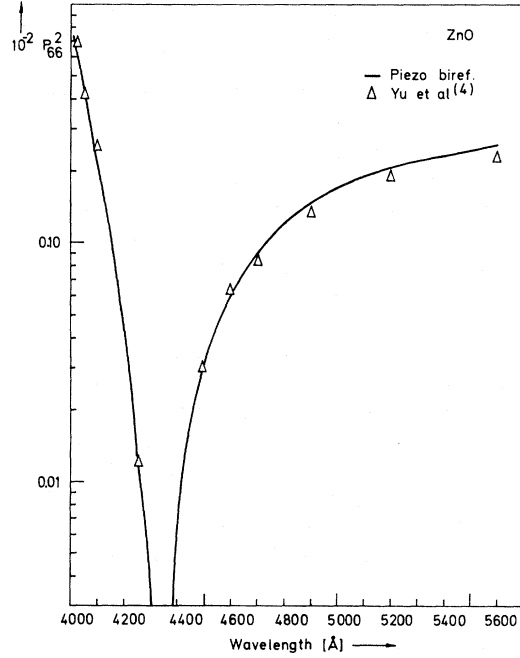


FIG. 4. p_{66}^2 for ZnO obtained from stress measurements (solid line). Results of Yu *et al.* are also shown (triangles). Wavelength of the resonant cancellation point is 4328 Å.

One (I_1) has the incoming light polarized along the c axis of the unstrained crystal. The other (I_{45}) has the incoming light polarized 45° away from the c axis. By taking the ratio

$$I_1/I_{45} = \tan^2 2\theta,$$

the photoelastic constant p_{44} can be obtained. This way of determining p_{44} is of course more inaccurate than the simple piezobirefringence measurements of p_{66} . It seems, however, to be the only way to determine p_{44} from static stress measurements.

The values of p_{44}^2 and p_{66}^2 as measured in these ways are also shown in Figs. 1–4 together with the Brillouin scattering results. It is seen that the dispersion of the p coefficients obtained in these two different ways agree closely, clearly indicating that the Brillouin scattering mainly is governed by elasto-optic effects.

The values obtained by Yu and Cardona⁴ have been recomputed in terms of p_{66} and are also shown in Figs. 2 and 4. There is good agreement between these two sets of experimental results. The He-Ne laser results for CdS⁵ are also shown in Figs. 1 and 2. These values are somewhat different from our results.

The comparison between the Brillouin scattering results and the stress-induced birefringence results is very useful since the photoelastic coefficients determine both effects. For example, the

resonant cancellation point of the Brillouin scattering simply corresponds to the isotropic point of the stress-induced birefringence. This is the spectral point where the elasto-optic effects vanish, namely, where the dielectric constant is independent of strain (up to first order). The strain in the crystal obtained from static stress and acoustical phonons is equivalent, whereas the strain from optical phonons involves deformations of the unit cell itself. Hence, one should expect rather different spectra for Brillouin and Raman scattering. It is therefore surprising that the Raman scattering from TO phonons in CdS⁷ has a cancellation point at the same wavelength as that from Brillouin scattering. In ZnO, Raman spectra have not yet been recorded in the region of the cancellation point of Brillouin scattering. Preliminary measurements⁸ on hexagonal ZnS yield an isotropic point for the piezobirefringence (in the p_{66} geometry) at 3600 Å. Brillouin and Raman spectra have not yet been recorded in this region. However, Raman spectra at longer wavelengths⁸ (corresponding to the p_{44} geometry) seem to indicate the presence of a cancellation point of about 8200 Å. At these wavelengths we did not observe any unusual piezobirefringence.

IV. THEORY

The resonant enhancement and cancellation of Brillouin and Raman scattering are often described in terms of Loudon's theory.⁹ Here the enhancement of the scattering is due to a dispersive contribution from the fundamental band gap, while the cancellation may occur if the contribution from nonresonant terms have the opposite sign. It is, however, more simple to derive the photoelastic coefficients from the theory of stress-induced birefringence. Piezobirefringence has been observed in many materials.^{4, 10-12} Generally, a strong dispersion in the induced birefringence is observed near the fundamental band gap. Materials with lowest direct gaps larger than about 0.7 eV exhibit a sign reversal in the piezobirefringence when approaching the gap. This may be understood in terms of the following model.¹² There are two contributions to the piezobirefringence. One from the lowest direct gap yielding the dispersion, and one from higher bands represented by an average gap (the Penn gap). It has been shown that the contribution from the average gap is expected to have the opposite sign¹² of the contribution from the lowest gap. If then the dispersion due to the lowest direct gap is strong enough, the stress-induced birefringence changes sign as the band gap is approached, giving rise to an isotropic point where the intensity of the Brillouin scattering has a minimum.

Yu and Cardona⁴ found that exciton effects must be taken into account when computing the piezobirefringence of II-VI compounds. They added a single oscillator representing the ground-state exciton to the ordinary parabolic band states in their model and obtained good fits to the spectra observed. However, they had troubles with the band contribution for the wurtzite materials and pointed out that one reason for this might be that the parabolic band singularity due to exciton effects might be sharpened. We have taken this effect into account in the present work, considering also the unbound continuum exciton states.

As shown in Appendix B, the dielectric constant may then be written (as the components of a tensor)

$$\epsilon_{ij} = \epsilon_{\infty ij} + \sum_{\alpha} f_{ij}^{\alpha}(E), \quad (7)$$

where

$$f_{ij}^{\alpha}(E) = \frac{K_1 P_{ij}^{\alpha}}{E_{x\alpha}^2 - E^2 - iE\Gamma_{x\alpha}} + \frac{K_2 P_{ij}^{\alpha}}{E + i\Gamma/2} \ln \frac{E_{g\alpha}}{E_{g\alpha} - E - i\Gamma/2}. \quad (7a)$$

Here α labels the three fundamental valence bands; E_x and E_g are the corresponding ground-state exciton and band-gap energy. Γ is the damping, $\epsilon_{\infty ij}$ the background dielectric constant, while $K_1 P_{ij}^{\alpha}$ and $K_2 P_{ij}^{\alpha}$ are strength parameters for ground-state exciton and continuum excitons plus band-to-band transitions, respectively. Both the strength parameters are proportional to P_{ij}^{α} , the p matrix element squared,

$$P_{ij}^{\alpha} = p_{c\alpha}^i p_{\alpha c}^j + p_{c\alpha}^j p_{\alpha c}^i (1 - \delta_{ij}). \quad (8)$$

Here $p_{c\alpha}^i$ is the p -matrix element for a transition from the conduction band c to the valence band α for light polarized along the i th direction.

From (3) and (7) the expression for the photoelastic constants is derived:

$$p_{mn} = \frac{-(1 + \delta_{kl})}{2\epsilon_{ii}\epsilon_{jj}} \left[\frac{\partial \epsilon_{\infty ij}}{\partial e_{kl}} + \sum_{\alpha} \left(\frac{1}{P_{ij}^{\alpha}} \frac{\partial P_{ij}^{\alpha}}{\partial e_{kl}} f_{ij}^{\alpha}(E) - \frac{\partial E_{g\alpha}}{\partial e_{kl}} g_{ij}^{\alpha}(E) \right) \right], \quad (9)$$

where

$$g_{ij}^{\alpha}(E) = \frac{2K_1 P_{ij}^{\alpha} E_{x\alpha}}{(E_{x\alpha}^2 - E^2 - iE\Gamma_{x\alpha})^2} + \frac{K_2 P_{ij}^{\alpha}}{E_{g\alpha}(E_{g\alpha} - E)}. \quad (10)$$

Here m and n are the usual contractions of the indices ij and kl , respectively, as shown in Eq.(3a).

In Appendix C a perturbation calculation is carried out for the strain-induced changes in strengths and energy gaps for the quasicubic model. The resulting six photoelastic coefficients are listed in Appendix C. Of importance for the present work are p_{44} and p_{66} :

$$p_{44} = (1/\epsilon_{11}\epsilon_{33})(K_{44} + (C_6/2\sqrt{2})F_{44}), \quad (11)$$

$$p_{66} = (1/\epsilon_{11}^2)(K_{66} + 2C_5F_{66}), \quad (12)$$

where F_{44} and F_{66} are the dispersive contributions from the direct gap and are given by Eq. (C10). C_5 and C_6 are the shear deformation potentials, while K_{44} and K_{66} are the constant contributions to the piezobirefringence from higher bands (the average band gap). It should be noted that the dispersion of p_{44} and p_{66} is (to first order in strain) only caused by changes in the oscillator strengths. Furthermore, only the shear deformation potentials C_5 and C_6 enter these expressions (in first order); so C_5 and C_6 , in principle, could be determined more accurately from piezobirefringence measurements than from energy shifts, where the shear deformation potentials yield nonlinear shifts.

Some useful approximate relations may be derived from the six photoelastic coefficients in Appendix C. If the crystal-field parameter Δ of the quasicubic model tends to zero, the crystal becomes isotropic. In that case only two independent photoelastic coefficients p_{11} and p_{12} exist:

$$p_{33} = p_{11}, \quad p_{13} = p_{31} = p_{12} \quad (13)$$

and

$$p_{44} = p_{66} = \frac{1}{2}(p_{11} - p_{12}).$$

Similarly, only two deformation potentials C_1 and C_2 exist. From (13) with $\Delta=0$ one obtains

$$C_3 \approx C_2 - C_1, \quad C_4 \approx -\frac{1}{2}C_3, \quad C_5 \approx -C_4, \quad C_6 \approx \sqrt{2}C_5. \quad (14)$$

These relations are similar to those derived by Bir *et al.*¹³ They yield useful information about signs and approximate magnitudes of the deformation potentials. Similarly, approximate relations between the contributions from higher bands are obtained,

$$K_{33} \approx K_{11}, \quad K_{13} \approx K_{31} \approx K_{12}, \quad K_{44} \approx K_{66} \approx \frac{1}{2}(K_{11} - K_{12}).$$

V. COMPARISON WITH EXPERIMENTAL RESULTS

The expressions (11) and (12) have been plotted in case of CdS in Figs. 5 and 6. The parameters involved are listed in Table I. All parameters connected with the ground state excitons are known and have been taken from the literature. $E_g - E_x$ should correspond to the exciton binding energy of 28 meV. Better agreement was, however, ob-

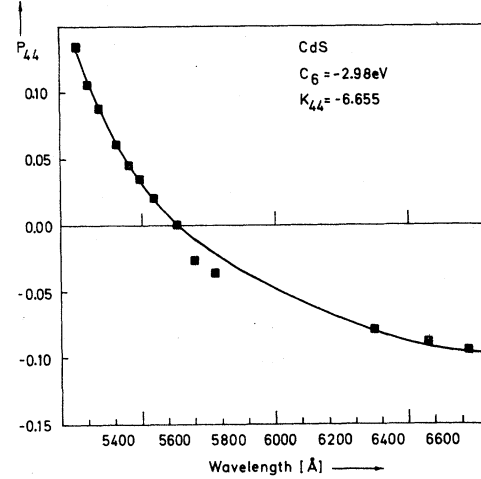


FIG. 5. p_{44} for CdS computed from Eq. (11) (solid line) and compared with the stress measurements (squares).

tained with $E_g - E_x = 44.5$ meV, which was then used for CdS. The only parameters obtained by fitting are marked by a star in Table I. They are the strengths of the continuum exciton states and band transitions and the background dielectric constants. These parameters were found by fitting Eq. (2) to the refractive indices known from the literature.¹⁴ In determining p_{66} (or p_{44}) only two parameters are left, the K_{66} and C_5 parameters (K_{44} , C_6). The K_{66} parameter (K_{44}) is determined from the zero in p_{66} (p_{44}) (which is well known since it corresponds to the isotropic point or the cancellation point of the Brillouin scattering). K_{66} (K_{44}) is the negative constant contribution from higher bands. p_{66} (p_{44}) is then proportional to C_5 (C_6), which may thus be determined by a mere scaling of the computed curve. This means that the rela-

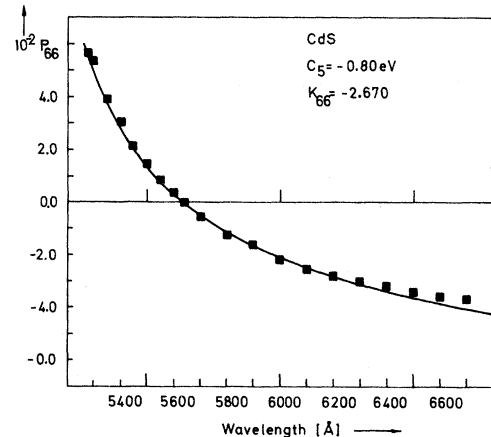


FIG. 6. p_{66} for CdS computed from Eq. (12) (solid line) compared with the stress measurements (squares).

TABLE I. Parameters used in the calculation of p_{66} and p_{44} for ZnO and CdS. The values marked by an asterisk are obtained from fitting to refractive indices.

	CdS	ZnO
E_{x1} (eV)	2.4727 ^a	3.306 ^d
E_{x2} (eV)	2.4876 ^a	3.306 ^d
E_{x3} (eV)	2.5510 ^a	3.340 ^d
$K_1 P_{xx}^1$ (eV ²)	0.072 ^c	0.15 ^e
$K_1 P_{xx}^2$ (eV ²)	0.040 ^c	0.30 ^e
$K_1 P_{zz}^2$ (eV ²)	0.044 ^c	0.0 ^e
$K_1 P_{xx}^3$ (eV ²)	0.022 ^c	0.0 ^e
$K_1 P_{zz}^3$ (eV ²)	0.048 ^c	0.38 ^e
$\Gamma_x = \Gamma$ (meV)	40 ^a	40 ^f
Δ (meV)	27.0 ^b	41 ^b
λ (meV)	21.7 ^b	-2.9 ^b
E_1 (eV)	2.5172	3.366
$K_2 P_x^2$ (eV ²)	2.470*	2.704*
$K_2 P_z^2$ (eV ²)	2.725*	3.153*
$\epsilon_{\infty \perp}$ ($E \perp c$)	4.132*	2.642*
$\epsilon_{\infty \parallel}$ ($E \parallel c$)	4.096*	2.524*

^a E. Gutsche and J. Voigt, in *Proceedings of the II-VI Semiconductor Compound Conference*, 1967, Brown University, edited by D. G. Thomas (Benjamin, New York, 1967), p. 337.

^b J. O. Dimmock, in *Proceedings of the II-VI Semiconductor Compound Conference*, 1967, Brown University (Benjamin, New York), p. 277.

^c D. G. Thomas and J. J. Hopfield, *Phys. Rev.* **116**, 573 (1959).

^d M. Cardona, K. L. Shaklee, and F. H. Pollak, *Phys. Rev.* **154**, 696 (1967).

^e Reference 19.

^f G. Hvedstrup Jensen, *Phys. Status Solidi B* **64**, K51 (1974).

tive values (the shape or dispersion) of p_{66} (or p_{44}) are computed essentially without any adjustable parameters. The agreement between the experimental results and the computed curve is thus very good.

There is nothing in the theory which indicates that the isotropic (or cancellation) point should be positioned at the same energy both for p_{44} and p_{66} . However, one might expect this on basis of the quasicubic model.¹⁵ When the crystal-field parameter $\Delta = 0$, then $p_{44} = p_{66}$. When $\Delta \neq 0$ a hexagonal strain field is present, but since the property of the isotropic point is its independence of strain (at least to first order), one should expect the isotropic point to be nearly common to p_{44} and p_{66} also when $\Delta \neq 0$. From Figs. 5 and 6 one obtains $C_5 = -0.80$ eV and $C_6 = -2.98$ eV (for CdS). Previous values obtained are $C_5 = -1.5,^{16} -1.2$ eV¹⁷ and $C_6 = -2.4,^{16} -1.1$ eV.¹⁷ The agreement is reasonable taking into account that C_5 and C_6 previously were determined from second-order energy shifts. The K values obtained are $K_{44} = -6.655$ and $K_{66} = -2.670$.

Similar results for p_{44} and p_{66} are shown for ZnO in Figs. 7 and 8. The parameters used here are listed in Table I. All parameters connected with the ground-state exciton are known and have been taken from the literature. $E_g - E_x$ was chosen to be 60 meV, which is the binding energy of the excitons.

The strength of the continuum states and the background dielectric constant were fitted to refractive indices taken from the literature.¹⁸ K_{66} , K_{44} , C_5 , and C_6 were obtained in the same way as for CdS. In case of ZnO, however, the exchange splitting j of the excitons is comparable to the spin-orbit splitting. This gives rise to pronounced changes in the oscillator strengths. As seen from Table I the oscillator strength of the A exciton is only half of that of the B exciton, although the one-electron band-to-band transitions for the A and B bands should have nearly equal strengths.

Yu and Cardona⁴ made an approximate calculation of the influence on p_{66} of exchange interaction between the ground-state excitons. Their correction was only a few percent. However, they used a wrong value of the exchange parameter for ZnO ($j = 5.6$ meV¹⁶). This value corresponds, essentially, to the splitting between the longitudinal excitons, since it was determined from the splittings of reflectivity minima, as pointed out in Ref. (19). It is the exchange splitting between transverse excitons which must be applied when determining resonance energies and oscillator strengths. The exchange parameter for the transverse excitons is $j = 0.95$ meV.¹⁹ With this value it is not possible to neglect the influence of the A

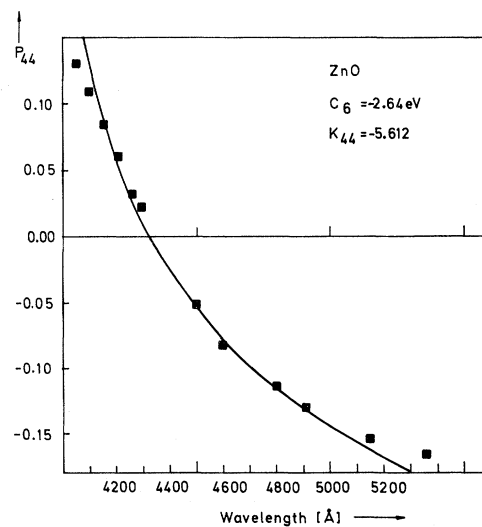


FIG. 7. p_{44} for ZnO computed from Eq. (11) (solid line) compared with the stress measurements (squares).

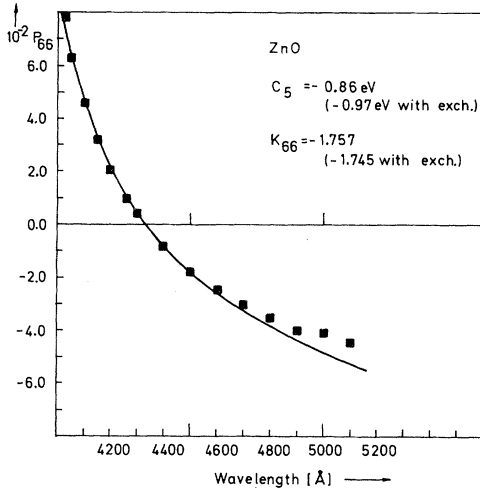


FIG. 8. p_{66} for ZnO computed from Eq. (12) (solid line) compared with the stress measurements (squares). Values of K_{66} and C_5 obtained with exchange interaction taken into account are also shown.

exciton as was done in Ref. (4), and the analysis becomes more involved. In Appendix C we have estimated the exchange effects by using the results of Ref. (19). It should be noted that there also exists exchange interaction between the continuum exciton states. However, the value of j is different for these. For simplicity, we use the same value of j for both bound and unbound states. The result obtained in Appendix C is that the exchange does not influence the dispersion of p_{66} appreciably, but only reduces the absolute values.

From Figs. 7 and 8 one obtains the K values $K_{44} = -5.612$ and $K_{66} = -1.757$. Furthermore, we find $C_5 = -0.86$ eV neglecting exchange and $C_5 = -0.97$ eV including exchange and $C_6 = -2.64$ eV. Thus it is not possible from the shape of the p_{66} curve to tell whether exchange effects are important or not (at least in the wavelength region considered here). Previous values of the shear deformation potentials are $C_5 = -1.2$,¹⁶ -1.2 ,¹⁹ and -1.24 eV²⁰ and $C_6 = -2.0$ eV.¹⁶ The agreement seems to be reasonable, since the previous values are determined from second-order terms.

VI. CONCLUSION

We have obtained the dispersion of p_{44} and p_{66} both from piezobirefringence and Brillouin scattering measurements and thus established that the Brillouin scattering in CdS and ZnO is determined by elasto-optic effects alone. The resonant enhancement and cancellation of the Brillouin scattering correspond to the dispersion in the stress-induced birefringence and its isotropic point, respectively. Expressions for the six independent

photoelastic coefficients were derived applying perturbation theory within the frame of the quasi-cubic model. Exciton effects have been taken properly into account. A model dielectric constant has been derived for a solid where both ground-state excitons and unbound continuum exciton states contribute. The shear deformation potentials of CdS and ZnO were obtained for the first time from linear expressions.

ACKNOWLEDGMENT

We wish to thank Dr. D. H. R. Price for his cooperation in the determination of p_{66} from Brillouin scattering.

APPENDIX A

From Eq. (3a) the following relations are obtained:

$$\Delta\epsilon_{11} = -\epsilon_{11}^2(p_{11}e_{11} + p_{12}e_{22} + p_{13}e_{33}), \quad (\text{A1})$$

$$\Delta\epsilon_{22} = -\epsilon_{11}^2(p_{12}e_{11} + p_{11}e_{22} + p_{13}e_{33}), \quad (\text{A2})$$

$$\Delta\epsilon_{33} = -\epsilon_{33}^2(p_{31}e_{11} + p_{31}e_{22} + p_{33}e_{33}), \quad (\text{A3})$$

$$\Delta\epsilon_{13} = -2\epsilon_{11}\epsilon_{33}p_{44}e_{13}, \quad (\text{A4})$$

when only the strain components e_{11} , e_{22} , e_{33} , and e_{13} are considered.

For uniaxial stress $X \perp c$ we have $e_{11} = S_{11}X$, $e_{22} = S_{12}X$, $e_{33} = S_{13}X$, and $e_{13} = 0$. When the light direction k is parallel to the c axis ($k \parallel c$), the important birefringence is

$$\begin{aligned} \Delta n &= \Delta n_2 - \Delta n_1 \approx (1/2\sqrt{\epsilon_{11}})(\Delta\epsilon_{22} - \Delta\epsilon_{11}), \\ \Delta n &= \frac{1}{2}\epsilon_{11}^{3/2}(p_{11} - p_{12})(e_{11} - e_{22}) = \frac{1}{2}\epsilon_{11}^{3/2}p_{66}S_{66}X, \end{aligned} \quad (\text{A5})$$

where

$$S_{66} = 2(S_{11} - S_{12}) \quad \text{and} \quad p_{66} = \frac{1}{2}(p_{11} - p_{12}).$$

When the uniaxial stress X forms the angle α with the c axis, the strain components are

$$e_{11} = (S_{12} \sin^2\alpha + S_{13} \cos^2\alpha)X, \quad (\text{A6})$$

$$e_{22} = (S_{11} \sin^2\alpha + S_{13} \cos^2\alpha)X, \quad (\text{A7})$$

$$e_{33} = (S_{13} \sin^2\alpha + S_{33} \cos^2\alpha)X, \quad (\text{A8})$$

$$e_{13} = \frac{1}{4}S_{44} \sin(2\alpha)X. \quad (\text{A9})$$

As seen from (A4) and (A9), the dielectric tensor is no longer diagonal. The new eigenvalues are

$$\begin{aligned} \lambda_{1,3} &= \frac{1}{2}(\epsilon_{11} + \epsilon_{33}) \pm \frac{1}{2}[(\epsilon_{11} - \epsilon_{33})^2 + 4\Delta\epsilon_{13}^2]^{1/2}, \\ \lambda_2 &= \epsilon_{11}. \end{aligned}$$

The new eigenvectors are

$$(1, 0, (\lambda_1 - \epsilon_{11})/\Delta\epsilon_{13}); (0, 1, 0);$$

$$((\epsilon_{11} - \lambda_1)/\Delta\epsilon_{13}, 0, 1).$$

The angle θ between the new optical axis and the old one is given by

$$\tan\theta = \frac{\lambda_1 - \epsilon_{11}}{\Delta\epsilon_{13}} = \frac{2\Delta\epsilon_{13}}{\epsilon_{11} - \epsilon_{33} + [(\epsilon_{11} - \epsilon_{33})^2 + 4\Delta\epsilon_{13}^2]^{1/2}},$$

or, more conveniently,

$$\tan 2\theta = \frac{2\Delta\epsilon_{13}}{\epsilon_{11} - \epsilon_{33}},$$

$$\tan 2\theta = \frac{4\epsilon_{11}\epsilon_{33}p_{44}\epsilon_{13}}{\epsilon_{33} - \epsilon_{11}} = \frac{\epsilon_{11}\epsilon_{33}p_{44}S_{44}(\sin 2\alpha)X}{\epsilon_{33} - \epsilon_{11}}. \quad (\text{A10})$$

APPENDIX B: DIELECTRIC CONSTANT FOR II-VI COMPOUNDS

In II-VI compounds the exciton transitions are relatively strong. Hence they must be considered when computing the dispersion of the refractive index. Yu and Cardona⁴ have done this by adding the contribution from an exciton oscillator to the dispersion from a parabolic band. In that treatment, however, the continuum states of the excitons are neglected. Since these states possess considerable strength, we shall include them in the present work.

The absorption $\alpha(E)$ due to exciton transitions has been derived by Elliott²¹ and may be written²²

$$\alpha(E) = \frac{K'}{N} \left(\sum_n \frac{2R_0\delta(E - E_n)}{n^3} + \frac{\Theta(E - E_g)}{1 - e^{-2\pi\alpha}} \right), \quad (\text{B1})$$

where R_0 is the ground-state exciton binding energy, E_n is the energy of the n th excited exciton state, E_g is the band-gap energy, $\Theta(E - E_g)$ is the unit step function, N is the refractive index at the energy E in question, while

$$Z^2 = \frac{R_0}{E - E_g} \quad \text{and} \quad K' = \frac{1}{\hbar c} \frac{\mu}{m_0} \frac{4\pi\epsilon_s R_0 P^2}{E_X}.$$

Here μ is the reduced exciton mass, m_0 is the free-electron mass, ϵ_s is the relative value of the static dielectric constant, and E_X is the ground-state exciton energy, while $P^2 = 2|\langle \bar{p} \rangle|^2 / 3m_0$. $\langle \bar{p} \rangle$ is the momentum matrix element for a transition from the valence to the conduction band.

From (B1) the imaginary part of ϵ_2 is found:

$$\epsilon_2 = \frac{\hbar c K'}{E} \left(\sum_n 2R_0 \frac{\delta(E - E_n)}{n^3} + \frac{\Theta(E - E_g)}{1 - e^{-2\pi\alpha}} \right). \quad (\text{B2})$$

The real part ϵ_1 may be found by Kramers-Kronig

transforming ϵ_2 . In order to perform this transformation we shall neglect the exponential in the denominator. This is a reasonable approximation since most of the transitions occur near the critical point $E \simeq E_g$. In our model, furthermore, we shall neglect the excited bound exciton states. The model dielectric constant then attains its contributions from the ground-state exciton and the unbound continuum exciton states:

$$\epsilon_2 = (K_1/E) \delta(E - E_x) + (K_2/E) \Theta(E - E_g), \quad (\text{B3})$$

where $K_1 = 2R_0\hbar eK'$ and $K_2 = K_1/2R_0$. However, we introduce an extra degree of freedom by letting K_2 be independent of K_1 . This is done because the one electron band-to-band transitions also contribute. By Kramers-Kronig transforming this expression we find

$$\epsilon_1 = \epsilon_\infty + \frac{K_1}{\pi E_x(E_x - E)} + \frac{K_2}{\pi E} \ln \left| \frac{E_g}{E_g - E} \right|,$$

where ϵ_∞ is the background dielectric constant arising from higher-energy bands. With $2E_x \simeq E_x + E$, we obtain the more conventional expression for the oscillator term,

$$\epsilon_1(E) = \epsilon_\infty + \frac{2K_1/\pi}{E_x^2 - E^2} + \frac{K_2/\pi}{E} \ln \left| \frac{E_g}{E_g - E} \right|.$$

Introducing a broadening Γ_x for bound excitons and Γ for the continuum states, the complex model dielectric constant may be written

$$\epsilon(E) = \epsilon_\infty + \frac{F}{E_x^2 - E^2 - iE\Gamma_x} + \frac{K_0}{E + i\Gamma/2} \ln \frac{E_g}{E_g - E - i\Gamma/2}, \quad (\text{B4})$$

where $F = 2K_1/\pi$ and $K_0 = K_2/\pi$. Equation (B4) forms the basis of the computations in the present work. For ZnO, where the exciton effects are most pronounced, we obtain from fitting to refractive indices that $K_0 = 2.70$ eV. If the exciton continuum states contributed alone to K_0 , one should expect $K'_0 = F/4R_0$. For ZnO, $F = 0.45$ eV² and $R_0 = 60$ meV; so $K'_0 = 1.9$ eV. This means that about $\frac{2}{3}$ of the K_0 strength arises from the unbound continuum states which then seem to contribute considerably to the dispersion of the refractive index. For these materials it may therefore be of limited value to apply the parabolic band model.⁴

APPENDIX C: PERTURBATION CALCULATION OF PHOTOELASTIC COEFFICIENTS

In the quasicubic model for wurtzite crystals¹⁵ the three p -valence bands are split by spin-orbit splitting (3λ) and crystal-field splitting (Δ). The corresponding three energies of the band gaps

involved are¹⁵

$$E_{2,3} = E_1 \pm \frac{1}{2}[(\Delta - \lambda)^2 + 8\lambda^2]^{1/2} + \frac{1}{2}(\Delta + 3\lambda), \quad (C1)$$

where E_1 is the width of the fundamental band gap. The wave functions of the three valence bands¹⁵ are given in Table II. Here the arrows indicate spin functions. $p_{\pm} = 2^{-1/2}(p_x \pm ip_y)$, and p_x , p_y , and p_z are basis functions for the p -valence bands with pure x , y , and z symmetry, respectively, while

$$\alpha_{\pm} = \frac{1}{2}\{1 \pm (\Delta - \lambda)/[(\Delta - \lambda)^2 + 8\lambda^2]^{1/2}\}. \quad (C2)$$

We use the strain Hamiltonian \hat{H}_s of Pikus.²³ The strain components e_{11} , e_{22} , e_{33} , and e_{13} are sufficient for determining the six independent photoelastic coefficients. The relevant matrix elements are

$$\begin{aligned} \langle p_x \uparrow | \hat{H}_s | p_x \uparrow \rangle &= \langle p_x \downarrow | \hat{H}_s | p_x \downarrow \rangle = \Lambda_1 - \Lambda_5, \\ \langle p_y \uparrow | \hat{H}_s | p_y \uparrow \rangle &= \langle p_y \downarrow | \hat{H}_s | p_y \downarrow \rangle = \Lambda_1 + \Lambda_5, \\ \langle p_x \uparrow | \hat{H}_s | p_z \uparrow \rangle &= \langle p_x \downarrow | \hat{H}_s | p_z \downarrow \rangle = -\Lambda_6, \\ \langle p_z \uparrow | \hat{H}_s | p_z \uparrow \rangle &= \langle p_z \downarrow | \hat{H}_s | p_z \downarrow \rangle = \Lambda_3. \end{aligned}$$

Here,

$$\begin{aligned} \Lambda_1 &= (C_1 + C_3)e_{33} + (C_2 + C_4)(e_{11} + e_{22}), \\ \Lambda_5 &= C_5(e_{11} - e_{22}), \\ \Lambda_3 &= C_1 e_{33} + C_2(e_{11} + e_{22}), \\ \Lambda_6 &= (1/\sqrt{2})C_6 e_{13}. \end{aligned}$$

Furthermore, it is convenient to introduce

$$\Lambda_4 = \Lambda_1 - \Lambda_3 = C_3 e_{33} + C_4(e_{11} + e_{22}).$$

Here $C_1 - C_6$ are the six independent deformation potentials for the p -valence bands of wurtzite structures. We obtain the energy gaps as functions of strain from a perturbation calculation up to second order:

$$\begin{aligned} E_1 &= E_1^0 + \Lambda_1 + \frac{\alpha_+ \Lambda_5^2}{E_{12}} + \frac{\alpha_- \Lambda_5^2}{E_{13}} + \frac{\alpha_- \Lambda_6^2}{2E_{12}} + \frac{\alpha_+ \Lambda_6^2}{2E_{13}}, \\ E_2 &= E_2^0 + \alpha_+ \Lambda_1 + \alpha_- \Lambda_3 - \frac{\alpha_+ \Lambda_5^2}{E_{12}} - \frac{\alpha_- \Lambda_6^2}{2E_{12}} \\ &\quad + \frac{\alpha_+ \alpha_- \Lambda_4^2}{E_{23}} + \frac{\Lambda_6^2}{2E_{23}}, \\ E_3 &= E_3^0 + \alpha_- \Lambda_1 + \alpha_+ \Lambda_3 - \frac{\alpha_- \Lambda_5^2}{E_{13}} - \frac{\alpha_+ \Lambda_6^2}{2E_{13}} \\ &\quad - \frac{\alpha_+ \alpha_- \Lambda_4^2}{E_{23}} - \frac{\Lambda_6^2}{2E_{23}}, \end{aligned} \quad (C3)$$

where $E_{1,2,3}^0$ are the unperturbed energies given by (C1), and $E_{12} = E_1^0 - E_2^0$, $E_{13} = E_1^0 - E_3^0$, and $E_{23} = E_2^0 - E_3^0$. These expressions have previously been derived by Rowe *et al.*¹⁷ In their derivation, however, there are errors of factors of 2 in their expressions for C_5 and C_6 . Denoting the shear de-

TABLE II. Wave functions of the quasicubic model.

E_1	E_2	E_3
$\psi_{1a} = p_x \uparrow$	$\psi_{2a} = \sqrt{\alpha_+} p_x \uparrow + \sqrt{\alpha_-} p_z \uparrow$	$\psi_{3a} = \sqrt{\alpha_-} p_x \uparrow - \sqrt{\alpha_+} p_z \uparrow$
$\psi_{1b} = p_x \downarrow$	$\psi_{2b} = \sqrt{\alpha_+} p_x \downarrow - \sqrt{\alpha_-} p_z \downarrow$	$\psi_{3b} = \sqrt{\alpha_-} p_x \downarrow + \sqrt{\alpha_+} p_z \downarrow$

formation potentials C_5 and C_6 of Rowe *et al.*¹⁷ by C_{5R} and C_{6R} the correct values are given by

$$C_5 = 2C_{5R} \text{ and } C_6 = \sqrt{2}C_{6R}.$$

From the perturbed wave functions we obtain the following expressions for the squared p -matrix elements P_{ij}^{α} [defined in (8)]:

$$\begin{aligned} P_{xx}^1 &= \frac{1}{2} p_x^2 (1 - 2\alpha_+ \Lambda_5/E_{12} - 2\alpha_- \Lambda_5/E_{13}), \\ P_{yy}^1 &= \frac{1}{2} p_y^2 (1 + 2\alpha_+ \Lambda_5/E_{12} + 2\alpha_- \Lambda_5/E_{13}), \\ P_{zz}^1 &= 0, \\ P_{xx}^2 &= \frac{1}{2} \alpha_+ p_x^2 (1 + 2\Lambda_5/E_{12} + 2\alpha_- \Lambda_4/E_{23}), \\ P_{yy}^2 &= \frac{1}{2} \alpha_+ p_y^2 (1 - 2\Lambda_5/E_{12} + 2\alpha_- \Lambda_4/E_{23}), \\ P_{zz}^2 &= \alpha_- p_z^2 (1 - 2\alpha_+ \Lambda_4/E_{23}), \\ P_{xx}^3 &= \frac{1}{2} \alpha_- p_x^2 (1 + 2\Lambda_5/E_{13} - 2\alpha_+ \Lambda_4/E_{23}), \\ P_{yy}^3 &= \frac{1}{2} \alpha_- p_y^2 (1 - 2\Lambda_5/E_{13} - 2\alpha_+ \Lambda_4/E_{23}), \\ P_{zz}^3 &= \alpha_+ p_z^2 (1 + 2\alpha_- \Lambda_4/E_{23}), \end{aligned} \quad (C4)$$

where p_x and p_z are the numerical values of the p -matrix elements for transitions from valence bands with pure x (or y) and z symmetry, respectively. These expressions are identical with those derived by Yu and Cardona.⁴ Finally, we need the following contributions to the off-diagonal elements of the dielectric constant:

$$\begin{aligned} P_{xz}^1 &= -p_x p_z \Lambda_6 (\alpha_-/E_{12} + \alpha_+/E_{13}), \\ P_{zx}^1 &= p_x p_z \Lambda_6 (\alpha_-/E_{12} - 1/E_{23}), \\ P_{xz}^3 &= p_x p_z \Lambda_6 (\alpha_+/E_{13} + 1/E_{23}). \end{aligned} \quad (C5)$$

It turns out that the exchange splitting j between the excitons in ZnO may be important. Inclusion of this effect will, in general, mean solution of a 12×12 perturbation matrix.¹⁶ Fortunately, $j \ll \lambda$ and Δ in CdS so that j may be neglected here. In ZnO, however, $j \approx \lambda$ while j and $\lambda \ll \Delta$. Here, the exchange effects are important, but because of the large Δ the problem is considerably simplified. It was solved by Skettrup and Balslev,¹⁹ and we quote the results here. In this approximation $\lambda/\Delta \ll 1$, so $\alpha_+ \approx 1$ and $\alpha_- \approx 0$. This also implies that these effects only play a role in connection with the C_5 deformation potential. The results are¹⁹

$$\begin{aligned}
P_{xx}^1 &= \frac{1}{2} p_x^2 [1 - (j - \Lambda_5)/N_-] , \\
P_{yy}^1 &= \frac{1}{2} p_x^2 [1 - (j + \Lambda_5)/N_+] , \\
P_{xx}^2 &= \frac{1}{2} p_x^2 [1 + (j - \Lambda_5)/N_-] , \\
P_{yy}^2 &= \frac{1}{2} p_x^2 [1 + (j + \Lambda_5)/N_+] ,
\end{aligned} \tag{C6}$$

where

$$N_{\pm} = [\lambda^2 + (j \pm \Lambda_5)^2]^{1/2} .$$

Furthermore, the exciton energies also split. The A and B exciton energies are given by¹⁹

$$E_1 = E_1^0 + \Lambda_1 + \lambda + j - N_+ ,$$

$$E_2 = E_2^0 + \Lambda_1 + \lambda + j + N_+ ,$$

where the upper and lower signs correspond to light polarized along or perpendicular to the stress direction, respectively.

The photoelastic coefficients may now be derived from Eq. (9). The following six independent coefficients exist:

$$\begin{aligned}
p_{11} &= (1/\epsilon_1^2)(K_{11} + 2C_5F_{66} - 2C_4F_1 + C_2G_x + C_4G'_x) , \\
p_{12} &= (1/\epsilon_1^2)(K_{12} - 2C_5F_{66} - 2C_4F_1 + C_2G_x + C_4G'_x) , \\
p_{13} &= (1/\epsilon_1\epsilon_3)(K_{13} - 2C_3F_1 + C_1G_x + C_3G'_x) , \\
p_{31} &= (1/\epsilon_1\epsilon_3)(K_{31} + 2C_4F_3 + C_2G_z + C_4G'_z) , \\
p_{33} &= (1/\epsilon_3^2)(K_{33} + 2C_3F_3 + C_1G_z + C_3G'_z) , \\
p_{44} &= (1/\epsilon_1\epsilon_3)[K_{44} + (C_6/2\sqrt{2})F_{44}] , \\
p_{66} &= \frac{1}{4}(p_{11} - p_{12}) = (1/\epsilon_1^2)(K_{66} + 2C_5F_{66}) .
\end{aligned}$$

Here, the K values are derivatives of the nondispersive-background dielectric constant as indicated in Eq. (9), $K_{66} = \frac{1}{2}(K_{11} - K_{12})$ and

$$F_1 = \frac{\alpha_- f_{xx}^2 - \alpha_+ f_{xx}^3}{E_{23}} ,$$

$$F_3 = \frac{\alpha_+ f_{zz}^2 - \alpha_- f_{zz}^3}{E_{23}} ,$$

$$F_{44} = p_x p_z \left(\frac{\alpha_-}{E_{12}} (a_1 - a_2) + \frac{\alpha_+}{E_{13}} (a_1 - a_3) + \frac{1}{E_{23}} (a_2 - a_3) \right) ,$$

$$F_{66} = \frac{\alpha_+ f_{xx}^1 - f_{xx}^2}{E_{12}} + \frac{\alpha_- f_{xx}^1 - f_{xx}^3}{E_{13}} ,$$

$$G_x = g_{xx}^1 + g_{xx}^2 + g_{xx}^3 , \quad G'_x = g_{xx}^1 + \alpha_+ g_{xx}^2 + \alpha_- g_{xx}^3 ,$$

$$G_z = g_{zz}^1 + g_{zz}^2 + g_{zz}^3 , \quad G'_z = g_{zz}^1 + \alpha_+ g_{zz}^2 + \alpha_- g_{zz}^3 ,$$

where f_{ij}^α , g_{ij}^α , and P_{ij}^α are given by (7), (10), and (C4)-(C6), while $a_i = f_{xz}^i/P_{xz}^i$.

In the case of ZnO, where exchange effects may be important, F_{66} is changed into

$$F'_{66} = \frac{1}{2} \left[B \left(\frac{f_{xx}^2}{1+A} - \frac{f_{xx}^1}{1-A} \right) + A(g_{xx}^1 - g_{xx}^2) \right] ,$$

where

$$A = \frac{j}{(\lambda^2 + j^2)^{1/2}} \quad \text{and} \quad B = \frac{\lambda^2}{(\lambda^2 + j^2)^{3/2}} .$$

It appeared from Appendix B that both the ground-state exciton and the continuum excitons are important for the dispersion of $\epsilon(E)$. Hence, we have included exchange effects for the continuum excitons as well. This must be an estimate, however, since j is different for these states.

It turns out that the first term in F'_{66} dominates over the second term in the relevant wavelength region. Remembering that for ZnO $E_{12} = -2(\lambda^2 + j^2)^{1/2}$, $\alpha_+ \simeq 1$, and $\alpha_- \simeq 0$, it is seen that F_{66} obtained with or without exchange interaction have exactly the same dispersion. In this approximation we have $F'_{66} \simeq F_{66} jB/A$; so the exchange interaction only changes the absolute values of p_{66} , but not the dispersion (in the wavelength region considered here).

*Work supported by Danish Natural Science Research Counsel (511-3721).

¹R. Berkowicz and D. H. R. Price, *Solid State Commun.* **14**, 195 (1974).

²J. F. Nye, *Physical Properties of Crystals* (Oxford U. P., London, 1960).

³B. Tell, J. M. Worlock, and R. J. Martin, *Appl. Phys. Lett.* **6**, 123 (1965).

⁴P. Y. Yu and M. Cardona, *J. Phys. Chem. Solids* **34**, 29 (1973).

⁵K. Wakita, M. Umeno, K. Takagi, and S. Miki, *J. Phys. Soc. Jpn.* **35**, 149 (1973).

⁶E. S. Kohn, *J. Appl. Phys.* **40**, 2608 (1969).

⁷J. M. Ralston, R. L. Wadsack, and R. K. Chang, *Phys. Rev. Lett.* **25**, 814 (1970) and T. C. Damen and J. F. Scott, *Solid State Commun.* **9**, 383 (1971).

⁸We wish to thank Prof. R. K. Chang for the opportunity of measuring piezobirefringence on the ZnS crystal he used for his Raman scattering experiments [J. L. Lewis, R. L. Wadsack, and R. K. Chang, in *Light Scattering in Solids*, edited by M. Balkanski (Flammarion, Paris, 1971), p. 41].

⁹R. Loudon, *Proc. R. Soc. Lond.* **A275**, 218 (1963).

¹⁰C. W. Higginbotham, M. Cardona, and F. H. Pollak, *Phys. Rev.* **184**, 821 (1969).

¹¹W. Wardzynski, *J. Phys. C* **3**, 1251 (1970).

¹²P. Y. Yu, M. Cardona, and F. H. Pollak, *Phys. Rev. B* **3**, 340 (1971).

¹³G. L. Bir, G. E. Pikus, L. G. Suslina, D. L. Fedorov, and E. B. Shadrin, *Fiz. Tverd. Tela* **13**, 3551 (1971) [*Soviet Phys.-Solid State* **13**, 3000 (1972)].

¹⁴H. Gobrecht and A. Bartschat, *Z. Phys.* **156**, 131

- (1959). T. M. Bieniewski and S. J. Czyzak, *J. Opt. Soc. Am.* 53, 496 (1963).
- ¹⁵J. J. Hopfield, *J. Phys. Chem. Solids* 15, 97 (1960).
- ¹⁶D. W. Langer, R. N. Euwema, K. Era, and T. Koda, *Phys. Rev. B* 2, 4005 (1970); sign of C_6 is corrected.
- ¹⁷J. E. Rowe, M. Cardona, and F. H. Pollak, *Proceedings of the II-VI Semiconductor Compound Conference, 1967*, Brown University, edited by D. G. Thomas (Benjamin, New York, 1967), p. 112. (C_5 and C_6 are corrected according to Appendix C).
- ¹⁸E. Mollwo, *Z. Angew. Phys.* 6, 257 (1954); W. L. Bond, *J. Appl. Phys.* 36, 1674 (1965).
- ¹⁹T. Skettrup and I. Balslev, *Phys. Status Solidi* 40, 93 (1970).
- ²⁰A. Gavini and M. Cardona, *Phys. Rev. B* 1, 672 (1970); C_5 corrected according to Appendix C.
- ²¹R. J. Elliott, *Phys. Rev.* 108, 1384 (1957).
- ²²D. D. Sell and P. Lawaetz, *Phys. Rev. Lett.* 26, 697 (1971).
- ²³G. E. Pikus, *Fiz. Tverd. Tela* 6, 324 (1964) [*Soviet Phys.-Solid State* 6, 261 (1964)].